The EMBO Journal (2010) 29, 884–896 | © 2010 European Molecular Biology Organization | All Rights Reserved 0261-4189/10
www.embojournal.org

THE EMBO JOURNAL

The PTB domain of ShcA couples receptor activation to the cytoskeletal regulator IQGAP1

Matthew J Smith[1], W Rod Hardy[2], Guang-Yao Li[1], Marilyn Goudreault[2], Steven Hersch[1], Pavel Metalnikov[2], Andrei Starostine[2], Tony Pawson[2,3,*] and Mitsuhiko Ikura[1,4,*]

[1]Division of Signaling Biology, Ontario Cancer Institute, MaRS TMDT, Toronto, Ontario, Canada, [2]Samuel Lunenfeld Research Institute, Mount Sinai Hospital, Toronto, Ontario, Canada, [3]Department of Molecular and Medical Genetics, University of Toronto, Toronto, Ontario, Canada and [4]Department of Medical Biophysics, University of Toronto, Toronto, Ontario, Canada

Adaptor proteins respond to stimuli and recruit downstream complexes using interactions conferred by associated protein domains and linear motifs. The ShcA adaptor contains two phosphotyrosine recognition modules responsible for binding activated receptors, resulting in the subsequent recruitment of Grb2 and activation of Ras/MAPK. However, there is evidence that Grb2-independent signalling from ShcA has an important role in development. Using mass spectrometry, we identified the multidomain scaffold IQGAP1 as a ShcA-interacting protein. IQGAP1 and ShcA co-precipitate and are co-recruited to membrane ruffles induced by activated receptors of the ErbB family, and a reduction in ShcA protein levels inhibits the formation of lamellipodia. We used NMR to characterize a direct, non-canonical ShcA PTB domain interaction with a helical fragment from the IQGAP1 N-terminal region that is pTyr-independent. This interaction is mutually exclusive with binding to a more conventional PTB domain peptide ligand from PTP–PEST. ShcA-mediated recruitment of IQGAP1 may have an important role in cytoskeletal reorganization downstream of activated receptors at the cell surface.

The EMBO Journal (2010) **29,** 884–896. doi:10.1038/emboj.2009.399; Published online 14 January 2010
Subject Categories: signal transduction; structural biology
Keywords: ErbB2; IQGAP1; lamellipodia; PTB domain; ShcA

Introduction

The Shc proteins are a family of adaptors containing N-terminal PTB and C-terminal SH2 domains (Ravichandran, 2001), each of which bind phosphorylated tyrosine (pTyr) residues in the context of specific amino acid sequences. ShcA is the most widely expressed of four mammalian Shc proteins, and its primary role is in signalling from activated receptors at the cell surface. These include receptors for growth factors (Ravichandran *et al*, 1995; Ricketts *et al*, 1996; Ganju *et al*, 1998; Meakin *et al*, 1999; Hennige *et al*, 2000; Finlayson *et al*, 2003; Motegi *et al*, 2004), antigens (Ravichandran *et al*, 1993; Pratt *et al*, 1999; Patrussi *et al*, 2005; Fukushima *et al*, 2006), and cytokines (Dorsch *et al*, 1994; Bates *et al*, 1998; Hunt *et al*, 1999), as well as integrins (Mainiero *et al*, 1995; Wary *et al*, 1996; Mauro *et al*, 1999; Cowan *et al*, 2000; Dans *et al*, 2001; Weyts *et al*, 2002) and GPCRs (Luttrell *et al*, 1997; Schafer *et al*, 2004; Natarajan and Berk, 2006). Recruitment of ShcA to assorted membrane proteins results in its phosphorylation on three tyrosine residues (Y239/40 and Y313) in a central CH1 domain that subsequently activate the Ras/MAPK pathway through the recruitment of Grb2 and SOS (Salcini *et al*, 1994; van der Geer *et al*, 1996).

PTB domain interactions typically mediate ShcA association with surface receptors. Selectivity is achieved through recognition of linear motifs with the consensus sequence Φ*X*NP*X*pY (Φ being a hydrophobic residue and *X* representing any amino acid) (Uhlik *et al*, 2005). A structure of the ShcA PTB domain complexed with a 12 residue phosphopeptide from the juxtamembrane of TrkA was solved by NMR spectroscopy (Zhou *et al*, 1995b). PTB domains, now identified in over 50 human proteins, share a similar core fold consisting of a central β-sandwich capped on one end by a conserved C-terminal α-helix, and on the other by a variable length α-helix found between strands β1 and β2 (or β2 and β3). The canonical peptide-binding groove is located between the fifth β-strand and the C-terminal α-helix (α3 in Shc); however, PTB domains possess surprisingly flexible binding properties including a variable dependence on phosphorylation of the NP*X*Y tyrosine (Uhlik *et al*, 2005). Numerous PTB domains (i.e. Dab or Numb) bind irrespective of phosphorylation or preferentially recognize unphosphorylated ligands, but members of the Shc and IRS-1/Dok families bind with higher affinity to phosphorylated motifs and serve as adaptors in normal and oncogenic receptor tyrosine kinase (RTK) signalling.

Although stimulation of the Ras pathway is a major component of Shc function, there are reasons to believe that Shc is involved in diverse processes. Though ShcA is an evolutionarily conserved protein, there is an intriguing absence of Y239/40 and Y313 tyrosines in more ancient orthologs. None of the three Shc-like proteins in nematodes contain these sites, and *Drosophila* Shc (dShc) has Y239/40 but not Y313; it is only in the chordate lineage that these are fixed. As Y313 appears to be the more potent Ras/MAPK activator, the absence of this phosphorylation site could limit the ability of dShc to stimulate the Ras/ERK pathway (Lai *et al*, 1995; Velazquez *et al*, 2000). These data imply a basic function for ShcA independent of its tyrosine

*Corresponding author. M Ikura, Department of Medical Biophysics and Division of Signaling Biology, University of Toronto and Ontario Cancer Institute, MaRS TMDT, 101 College Street, Toronto, Ontario, Canada M5G 1L7. Tel.: +1 416 581 7550; Fax: +1 416 581 7564;
E-mail: mikura@uhnresearch.ca or T Pawson, Department of Molecular and Medical Genetics, University of Toronto and Samuel Lunenfeld Research Institute, Mount Sinai Hospital, 600 University Avenue, Toronto, Ontario Canada, M5G 1X5. Tel.: +1 416 586 8262; Fax: +1 416 586 8869; E-mail: pawson@mshri.on.ca

Received: 10 July 2009; accepted: 10 December 2009; published online: 14 January 2010

phosphorylation, association with Grb2, or activation of MAPK. In support of this idea, ShcA has been reported to regulate c-Myc expression (Gotoh *et al*, 1997), play a role in cell survival (Gotoh *et al*, 1996), and control aspects of cytoskeletal architecture (Khoury *et al*, 2001).

Mice lacking ShcA die at E11.5 with cardiovascular defects, including lack of cardiac trabeculation, deficiencies in angiogenesis, and maintenance between endothelial and mesenchymal cell contacts (Lai and Pawson, 2000). Whole mount immunostaining also revealed a loss of MAPK activity using pERK antibodies. However, recent work has shown that a significant fraction of transgenic mice expressing ShcA proteins in which Y239/40 and Y313 have been replaced with phenylalanine (henceforth referred to as ShcA^{3F}) are viable (Hardy *et al*, 2007). Though *ShcA*$^{3F/3F}$ mice that live to adulthood exhibit severe ataxia, this is a much milder phenotype than that observed for mice expressing ShcA lacking PTB domain function (E11.5 lethal, similar to *ShcA*$^{-/-}$). These results support the notion that the central pTyr motifs in ShcA are dispensable for some of its biological activity, and hint that ShcA may have entirely independent signalling properties.

To search for unidentified pathways in the ShcA signalling network, we took a mass spectrometry-based approach to isolate new binding proteins. In this paper we show that ShcA interacts with the versatile scaffolding protein IQGAP1 (IQ-motif containing with homology to RasGAPs). This interaction is mediated through the ShcA PTB domain via a non-canonical binding mode, and we provide evidence that ShcA and IQGAP1 function downstream of activated receptors.

Results

Identification of novel ShcA-binding proteins

To begin exploring alternative pathways of ShcA signalling, we used a mass spectrometry-based approach to reveal unidentified binding partners. As bait, Flag-tagged wild-type p52 ShcA or ShcA^{3F} were stably expressed in Rat1 fibroblasts (Figure 1A) . The 3F protein carries Tyr-to-Phe mutations in the three CH1 domain residues that are targets for Grb2 (Y239/40 and Y313). We co-expressed in these cells an activated RTK ErbB2-YD, which carries a V664E mutation in the transmembrane region that increases homodimerization (Bargmann and Weinberg, 1988), and has only the ShcA PTB domain-binding site in the C-terminal tail (as defined by Dankort *et al*, 1997). This induced a transformed phenotype to these fibroblasts (Figure 1B). Proteins bound to ShcA after immunoprecipitation were separated by SDS–PAGE and stained with colloidal coomassie (Figure 1C). Cells expressing ErbB2-YD alone were used as a control. Proteins that associated specifically with both wild type and ShcA^{3F} were excised and identified by tandem mass spectrometry (LC-MS–MS). A protein of 197 kDa, equally visible in precipitations of both mutant and wild-type ShcA, was identified as IQGAP1. No IQGAP1 peptides were found from a corresponding region of the control lane. IQGAP1 is known to affect MEK/ERK activation (Roy *et al*, 2005) and has been linked to growth factor signalling and cytoskeletal rearrangements (Yamaoka-Tojo *et al*, 2004; Bensenor *et al*, 2007). Thus, we sought to further confirm this interaction and determine whether it was significant to ShcA signalling.

Verification of an ShcA interaction with IQGAP1

To validate the mass spectrometry result, we tested whether ShcA and IQGAP1 could be co-purified from Rat1 fibroblasts. We used wild-type Rat1 cells grown in standard media (10% serum), cells starved overnight and stimulated with EGF, or cells stably expressing ErbB2-YD. As several IQGAP1 interactions are mediated by Ca^{2+}/calmodulin, we also grew cells in media either lacking or supplemented with Ca^{2+} (Figure 1D). After the immunoprecipitation of endogenous Shc, we observed co-precipitation of IQGAP1 from all conditions (Figure 1D). Subsequently, we tested the requirement for the CH1 domain residues Y239/40 and Y313 using HEK 293T cells co-transfected with HA-tagged IQGAP1 and Flag-tagged wild type or 3F ShcA. IQGAP1 was co-precipitated with both proteins (Figure 1E). These data corroborate an interaction, provide evidence that the Shc CH1 tyrosines are not required for association with IQGAP1, and indicate that ErbB2 activity is not strictly required for formation of the complex.

Membrane recruitment of ShcA and IQGAP1

We next considered whether ShcA and IQGAP1 interact in cells. ShcA is generally cytoplasmic or ER localized, and is re-distributed upon receptor activation to the cell surface (Lotti *et al*, 1996). IQGAP1 is found in a Ca^{2+}-regulated complex with calmodulin (Ho *et al*, 1999), but in multiple cell types can accumulate at the leading edge of migrating cells (Mataraza *et al*, 2003, 2007; Watanabe *et al*, 2004; Yamaoka-Tojo *et al*, 2004). We initially utilized the Rat1 cell lines expressing ErbB2-YD and EGFP/Flag-ShcA (Figure 1A and B). The ErbB2-YD receptor is able to signal downstream through ShcA, but unlike wild-type ErbB2 has no direct Grb2-binding sites (Dankort *et al*, 1997, 2001). Wild-type cells showed pools of endogenous IQGAP1 localized generally in the cytoplasm, as well as to the cell cortex in cells nearing the edge of a monolayer (Figure 2A). However, we observed a clear loss of cytoplasmic IQGAP1 and its substantial recruitment to membrane ruffles along the leading edges of cellular protrusions in those cells which express ErbB2-YD and EGFP-ShcA. Although we detected exogenously expressed EGFP-ShcA or EGFP-ShcA^{3F} in these regions, they also remained prominent throughout the cytoplasm. In contrast to IQGAP1, a control protein that is also cytoplasmic in unstimulated cells (GAPDH) was not significantly recruited to membrane ruffles (Figure 2B). As ErbB2-YD signals through ShcA, these data signified that receptor activation may promote a ShcA interaction with IQGAP1 that is not dependant on the phosphorylation of its CH1 tyrosines.

To address the dependence of IQGAP1 localization on exogenously expressed ShcA, wild-type Rat1 cells were immunostained for the endogenous proteins (Figure 2C). Both IQGAP1 and Shc were generally cytoplasmic in unstimulated cells, particularly localized in the perinuclear region (with IQGAP1 also in the cell cortex in cells nearing the edge of a monolayer). We then examined cells expressing ErbB2-YD, and once more found IQGAP1 in membrane regions, wherein it co-localized with a fraction of Shc. The Shc proteins remained prominent throughout the cytoplasm. Finally, we monitored the effect of EGF on IQGAP1 and Shc localization in wild-type fibroblasts. After 20 min of stimulation, Shc was clearly detected in EGF-induced endosomes (see also Supplementary Figure S1A).

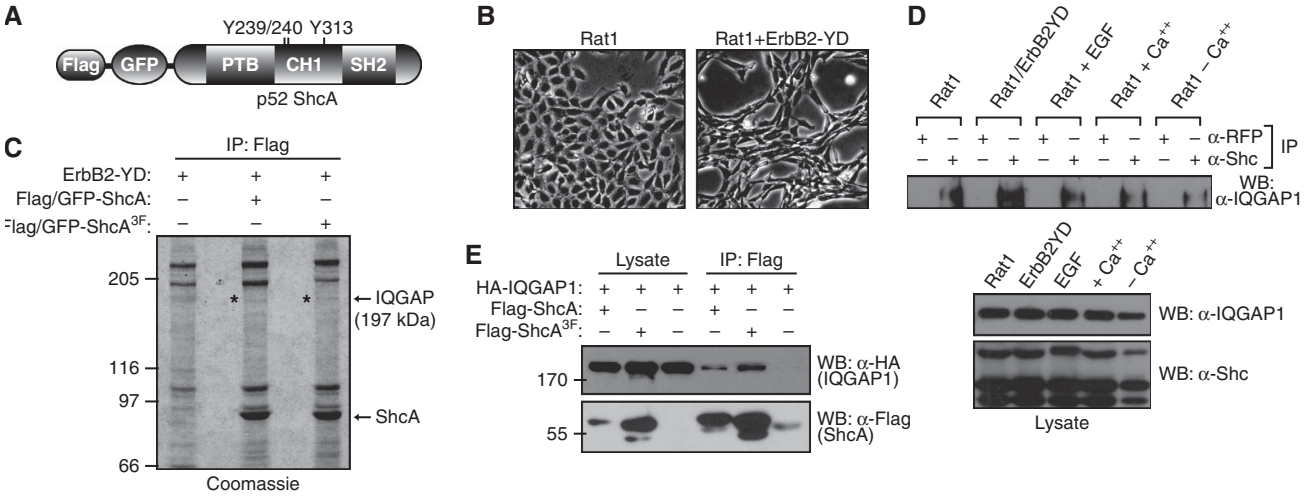

Figure 1 Identification and verification of IQGAP1 as an ShcA-binding protein. (**A**) Schematic diagram of ShcA proteins used as bait for mass spectrometry-based analysis. p52 isoform of ShcA was tagged with a Flag-GFP sequence at its N-terminus. (**B**) Rat1 fibroblasts containing activated ErbB2 exhibit characteristics of transformation, and were used to produce recombinant ShcA proteins. Cells stably expressing ErbB2 (right) no longer display contact inhibition like wild-type cells (left). (**C**) Proteins interacting with ShcA were identified by mass spectrometry. Immunoprecipitation of ShcA (lane 2) or ShcA^{3F} (lane 3) with anti-Flag antibodies was used to isolate bound proteins. Cells expressing only ErbB2 were used as control (lane 1). Precipitated proteins were detected with colloidal coomassie. Position of 197 kDa IQGAP1 is marked. (**D**) Endogenous IQGAP1 and ShcA co-precipitate in Rat1 cells. Anti-Shc antibodies were used to immunoprecipitate ShcA. Anti-RFP antibodies served as a control. Cells were grown in standard media, were stimulated with EGF, grown in the absence/presence of extracellular Ca^{2+}, or were stably expressing ErbB2. Immunoblotting with anti-Shc or anti-IQGAP1 determined expression levels (bottom). IQGAP1 precipitated by ShcA or controls was detected with anti-IQGAP1 (top). (**E**) Recombinant IQGAP1 co-precipitates with wildtype and 3F ShcA. HA-tagged IQGAP1 was co-expressed with Flag-tagged ShcA in HEK 293T cells. Immunoprecipitation with anti-Flag antibodies and immunoblotting with anti-HA revealed co-precipitated IQGAP1 (top). Anti-Flag immunoblot confirmed ShcA protein expression (bottom).

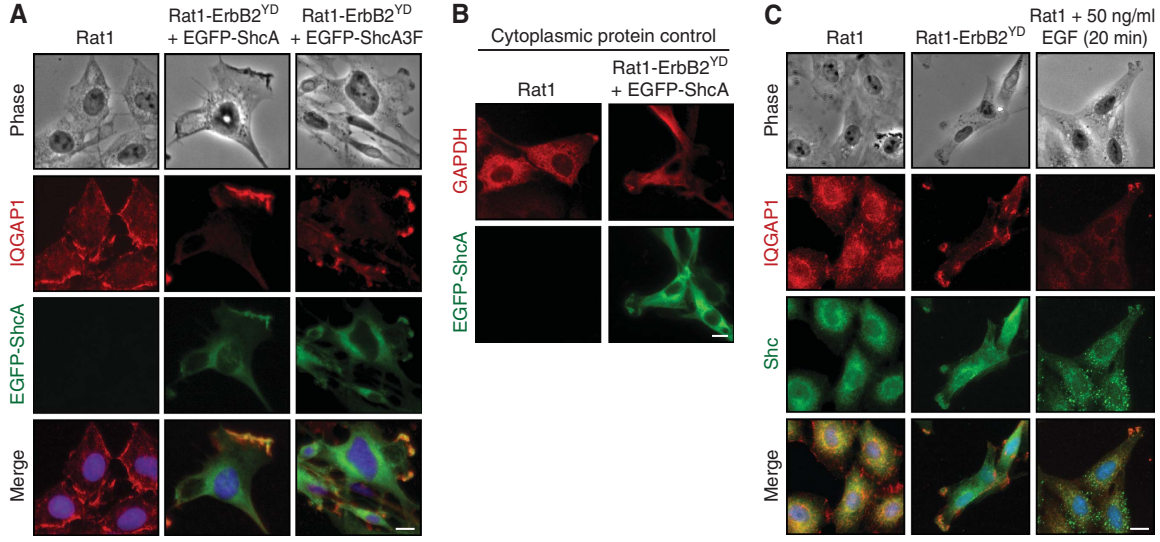

Figure 2 ShcA and IQGAP1 localization in Rat1 fibroblasts. (**A**) Cells stably expressing ErbB2-YD and EGFP-ShcA (green) were stained for endogenous IQGAP1 (red). Wild-type cells (column 1) served as a control. Merged images (bottom panels) show overlapping regions in yellow. Membrane ruffles are clearly seen in phase images (top panels). Bar = 10 μm. (**B**) A control cytoplasmic protein, GAPDH, still resides in the cytoplasm in cells expressing ErbB2-YD. Rat1 cells were stained with antibody against endogenous GAPDH (red). Both wild-type cells (column 1) and those expressing ErbB2-YD and EGFP-ShcA (green; column 2) show GAPDH localized throughout the cytoplasm. Bar = 10 μm. (**C**) IQGAP1 is also localized to membrane regions with endogenous ShcA. Cells were stained with anti-IQGAP1 (red) and antibody against endogenous Shc (green). Shc and IQGAP1 are generally cytoplasmic in wildtype cells grown in standard media (column 1), or are localized to membrane ruffles induced by expression of ErbB2-YD (column 2) or stimulation with EGF (column 3). Merged images (bottom panels) show overlapping localizations in yellow. Bar = 10 μm.

It is interesting to note that IQGAP1 was not observed in these punctate vesicles and remained in the cytoplasm as well as concentrated at membrane ruffles. This evidence suggested that IQGAP1 membrane recruitment by activated receptors does not require the overexpression of ShcA, and that IQGAP1 does not interact with ShcA after receptor internalization.

IQGAP1 has a role in regulating epithelial cell junctions that is distinct from its activity in fibroblasts (Kuroda *et al*, 1998). We therefore chose to examine ShcA and IQGAP1 in 5637 bladder carcinoma cells, which show moderate but stable cell–cell contacts (Supplementary Figure S1B). Although IQGAP1 showed a basolateral distribution in these cells (similar to E-cadherin or β-catenin), Shc was localized in

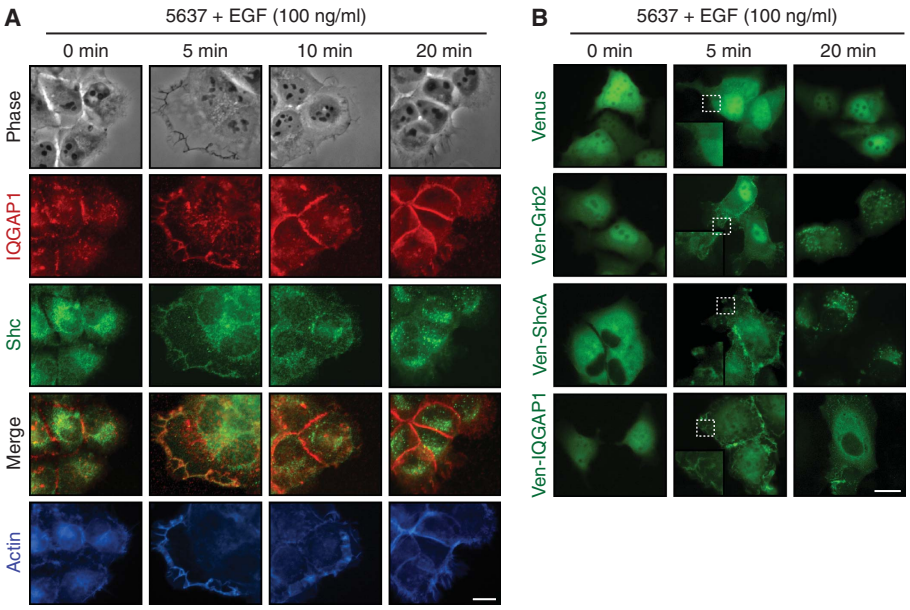

Figure 3 EGFR activation results in ShcA and IQGAP1 recruitment to membrane ruffles in 5637 epithelial cells. (**A**) Cells were stained for endogenous IQGAP1 (red) or Shc (green), along with actin (blue). 5 min after EGF stimulation massive ruffling was observed along the border of 5637 monolayers (column 2), subsiding after 10–15 min (column 3). ShcA is observed in EGFR-containing endosomes at 20 min mark (column 4). Bar = 10 μm. (**B**) Exogenously expressed ShcA, IQGAP1, and Grb2 show similar activity during the early stages of EGF stimulation. Venus-tagged proteins, as well as Venus alone, were expressed in 5637 cells, where they are localized throughout the cytoplasm and nucleus (apart from ShcA, which is not detected in the nucleus; column 1). Cells were EGF stimulated for 5 min (column 2) or 20 min (column 3). Grb2, Shc, and IQGAP1 all showed early membrane localization, whereas the Venus control protein did not. Only Grb2 and ShcA were detected in EGF-containing endosomes at 20 min. Bar = 10 μm.

the cytoplasm. Stimulation of these highly metastatic cells with EGF-induced rapid and extensive membrane ruffling around the edges of the monolayer. Immunostaining for IQGAP1 and ShcA revealed their presence in these lamellipodia, along with actin, after 5 min of EGF treatment (Figure 3A). Similar results were obtained in the A431 skin carcinoma cell line (Supplementary Figure S1C), but not with MDCK cells in which EGF-induced membrane ruffling was notably diminished or even absent (Supplementary Figure S2). Previous work has demonstrated similar dynamics upon EGF stimulation for fluorescently tagged Grb2 adaptor proteins (Sorkin *et al*, 2000), and to some extent ShcA (Sato *et al*, 2000). We consequently tested whether exogenously expressed, Venus-tagged IQGAP1 could be recruited to membranes upon EGF stimulation in 5637 cells. Indeed, although Grb2, ShcA, IQGAP1, and the Venus control are equally localized throughout the cytoplasm in unstimulated cells, only the Grb2, ShcA, and IQGAP1 proteins demonstrated clear membrane recruitment 5 min after the addition of EGF (Figure 3B). The Venus control remained cytoplasmic and displayed no or very little localization to the membrane. Moreover, we once more failed to observe IQGAP1 in the punctate endosomal vesicles that are evident in ShcA or Grb2 expressing cells following 20 min of EGF stimulation. This work corroborates our biochemical data, and establishes ShcA and IQGAP1 co-recruitment to membrane regions in both fibroblast and epithelial cell lines.

To further explore the role of ShcA in recruiting IQGAP1 to the cell cortex, we examined cells with reduced levels of ShcA protein for changes in IQGAP1 localization. Clonal lines of 5637 cells stably expressing shRNA against all three isoforms of ShcA were established, along with control lines expressing a scrambled shRNA sequence (Figure 4A). These cells were subjected to a time course of EGF stimulation, and control cells exhibited strong lamellipodia formation 5 min post-induction, in a manner analogous to wild-type cells. However, cells with reduced levels of ShcA showed greatly diminished levels of membrane ruffling, in most cases presenting no perceptible lamellipodia (Figure 4B and Supplementary Figure S3A). To determine whether IQGAP1 was still being recruited to the outer cortex in ShcA-knockdown cells, we immunostained these cell lines with antibodies against endogenous IQGAP1. Though control cells clearly retained the capacity to recruit IQGAP1 to membrane ruffles, there was no detectable change in IQGAP1 localization in ShcA-reduced cells upon stimulation with EGF (Figure 4C). Even treatment with significantly higher concentrations of EGF (100 ng/ml) failed to induce strong membrane ruffling in ShcA-knockdown cells (Supplementary Figure S3B/C). This lack of lamellipodia formation in ShcA-depleted cells likely correlates with a decrease in Rac1 activity. The loss of IQGAP1 has been highly associated with reduced migration in numerous cell types, and it is a powerful effector of Rac1 (Mataraza *et al*, 2003; Noritake *et al*, 2004; Watanabe *et al*, 2004). These data support a role for ShcA in recruiting IQGAP1 to membrane proximal regions in growth factor-stimulated cells.

Establishment of binding requirements for the ShcA–IQGAP1 complex

Previous reports have shown that IQGAP1 is tyrosine phosphorylated upon stimulation with EGF, PDGF, or VEGF (Blagoev *et al*, 2004; Yamaoka-Tojo *et al*, 2004; Kratchmarova *et al*, 2005), suggesting that IQGAP1 could directly associate

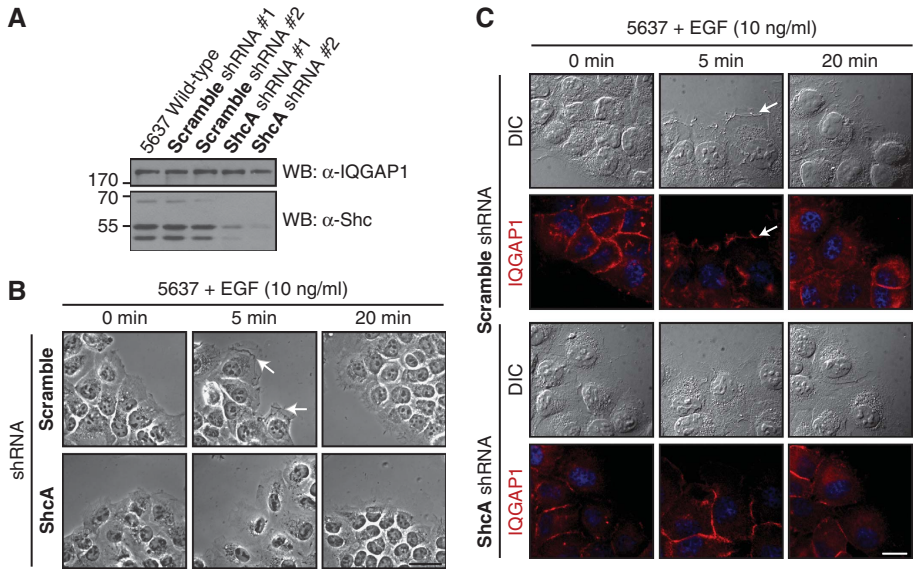

Figure 4 Reduction in ShcA protein levels leads to a loss of EGF-stimulated lamellipodia formation and IQGAP1 membrane recruitment. (**A**) Vector-based shRNA sequences directed against all three isoforms of ShcA were stably expressed in 5637 cells. Lysates from wild-type cells, as well as expanded clonal lines expressing either 'scrambled' shRNA control or shRNA against ShcA were immunoblotted with anti-Shc antibodies to determine protein levels (bottom). Probing with anti-IQGAP1 (top) served as a loading control and to ensure its level expression. Two lines for both the control and ShcA knockdown are shown. (**B**) 5637 cells with reduced levels of ShcA do not exhibit strong membrane ruffling. Control and ShcA knockdown lines were stimulated with 10 ng/ml EGF for 0, 5, or 20 min. Phase contrast images demonstrate a clear induction of lamellipodia in control cells at 5 min (middle, arrows). Similar results were obtained on multiple clonal cell lines. Bar = 40 μm. (**C**) Control and ShcA knockdown cells were stained for endogenous IQGAP1 (red) to establish its localization upon EGF stimulation. As with wild-type cells, 5 min after addition of EGF membrane ruffles containing IQGAP1 were observed in the control (top). These regions are clearly visible in DIC images and are marked by arrows. ShcA knockdown lines were highly deficient in lamellipodia formation and IQGAP1 was subsequently not recruited to the cell cortex (bottom). Bar = 10 μm.

with the ShcA PTB or SH2 domain. To begin examining this, we first chose to study IQGAP1 phosphorylation and its relationship with ShcA. We have detected a basal IQGAP1 tyrosine phosphorylation using anti-pTyr antibodies (Figure 5A). To determine whether phosphorylation is further stimulated by RTKs, we monitored IQGAP1 pTyr levels in cells expressing ErbB2-NT (carrying the V664E activating mutation and all five C-terminal pTyr sites; as defined in Dankort *et al* (1997)). Not only was IQGAP1 phosphorylation significantly increased by ErbB2, but overexpression of ShcA could further augment this (Figure 5B). Moreover, there was an enhanced capacity for hyperphosphorylated IQGAP1 to co-precipitate ShcA compared to IQGAP1 with only basal levels of phosphorylation. These data support a relationship between IQGAP1 pTyr levels and its interaction with ShcA, but do not yet clarify whether the PTB or SH2 domains might mediate a direct interaction.

To map the IQGAP1-binding site, we carried out a series of *in vitro*-binding experiments. GST-tagged ShcA PTB and SH2 domains were expressed and purified from *Escherichia coli*. Glutathione beads carrying the recombinant domains were incubated with cell lysates expressing HA-tagged IQGAP1, and co-precipitating proteins were identified by anti-HA immunoblot. Though both domains consistently pulled down IQGAP1, the PTB domain interaction was considerably more robust (Figure 5C). This experiment is complicated by the ability of IQGAP1 to oligomerize, as well as its affinity for actin and microtubules (Bashour *et al*, 1997; Fukata *et al*, 2002; Ren *et al*, 2005). We therefore sought to narrow the region of IQGAP1 targeted by ShcA using a set of truncation mutants (Figure 5D) and Far Western analysis. IQGAP1 fragments expressed and purified as HA-tagged proteins were separated by SDS–PAGE and transferred to a nitrocellulose membrane. The resulting membranes were incubated with GST-tagged PTB or SH2 domain, and direct interactions detected by anti-GST immunoblot (Figure 5E). Even though we observed no binding between IQGAP1 and the SH2 domain of ShcA (or GST alone), the PTB domain bound every fragment except ΔN. This suggested a direct interaction between the ShcA PTB domain and the N-terminal half of IQGAP1, in a region upstream of the WW domain.

In order to further categorize the binding site, we expressed and purified a series of GST-tagged fragments covering the entire N-terminal region (IQGAP1 residues 1–641). These were mixed with Ni-NTA beads carrying His-tagged PTB domain (or SH2 domain as a control), and bound proteins were identified by anti-GST immunoblot (Figure 6A). One fragment, spanning residues 401–533 of IQGAP1 (henceforth referred to as IQGAP1$^{401-533}$), was consistently precipitated by the PTB domain, whereas none interacted with SH2 domain. Unexpectedly, the interaction occurred directly after purification from *E. coli*, or with pre-incubation in EGF-activated cell lysates (not shown). This indicated that ShcA associates with IQGAP1 residues 401–533 even in the absence of tyrosine phosphorylation. As this is a non-canonical interaction for the ShcA PTB domain, we sought to further describe the binding mode.

NMR characterization of the PTB domain interaction with IQGAP1$^{401-533}$

ShcA is considered to have an archetypal pTyr-dependent PTB domain, but many PTB domains recognize motifs with a

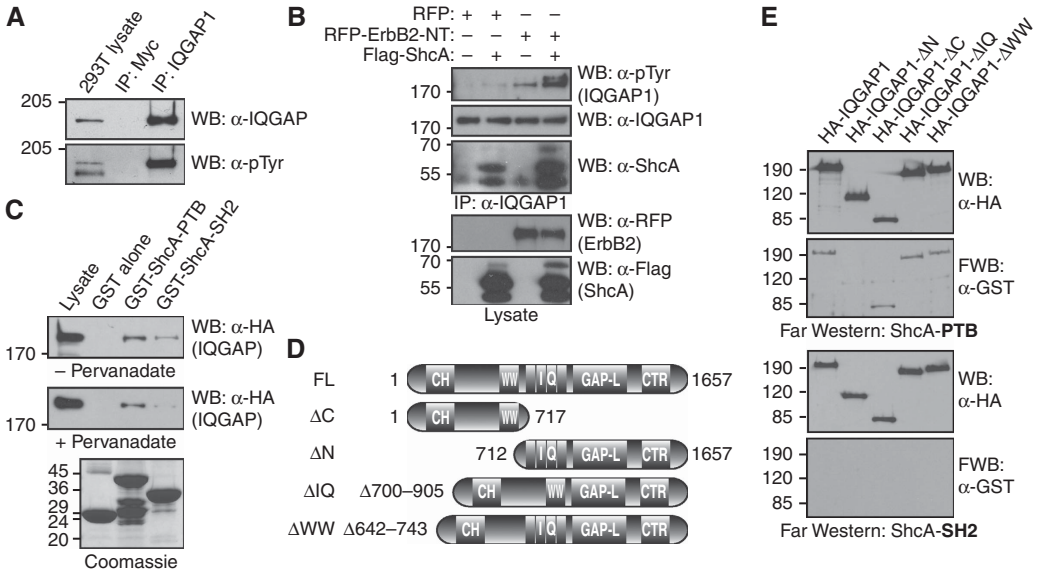

Figure 5 IQGAP1 is tyrosine phosphorylated and interacts directly with the ShcA PTB domain. (**A**) IQGAP1 is tyrosine phosphorylated in HEK 293T cells. Endogenous IQGAP1 was precipitated with anti-IQGAP1, and immunoblotting with anti-pTyr revealed phosphorylation (bottom panel). Anti-IQGAP1 immunoblot confirmed protein level (top panel), and precipitation with anti-Myc served as control. (**B**) Overexpression of ShcA induces phosphorylation of IQGAP1 in cells expressing activated ErbB2. Flag-tagged ShcA was co-expressed in HEK 293T cells with RFP-tagged ErbB2-NT or RFP alone as control. pTyr levels were determined by anti-pTyr immunoblot after immunoprecipitation of endogenous IQGAP1 (IP: top). Western blotting with anti-IQGAP1 confirmed protein levels (IP: middle), and with anti-Shc to determine co-precipitation (IP: bottom). Immunoblots of cell lysates with anti-RFP confirmed expression of ErbB2 (Lysate: top), while anti-Flag verified ShcA expression (Lysate: bottom). (**C**) Both the SH2 and PTB domains of ShcA precipitate full-length IQGAP1 from cell lysates. Recombinant domains were expressed in *Escherichia coli* as GST-fusion proteins, along with GST as a control. A coomassie stained gel shows loading of the purified proteins (bottom). HA-tagged IQGAP1 was expressed in HEK 293T cells, and GST pull downs performed with purified domains bound to glutathione beads. Precipitated IQGAP1 was identified by anti-HA immunoblot (top). Cells were also stimulated with the phosphatase inhibitor pervanadate for 30 min to induce tyrosine phosphorylation (middle). (**D**) Schematic showing IQGAP1 truncations. Fragments of IQGAP1 lacking the C-terminus (ΔC), the N-terminus (ΔN), the IQ motifs (ΔIQ), or the WW domains (ΔWW) were cloned and expressed with HA tags. Amino acid numbers are indicated according to murine IQGAP1. (**E**) The PTB domain of ShcA directly interacts with the N-terminal region of IQGAP1. Constructs expressing full-length IQGAP1, or the truncations, were expressed in HEK 293T cells. Proteins were immunoprecipitated with anti-HA and transferred to nitrocellulose membrane. Probing with GST–SH2 domain and anti-GST antibodies revealed no direct interactions (bottom panels). The PTB domain bound all truncations except ΔN (top panels). Reprobing with anti-HA confirmed expression of the IQGAP1 fragments (top panels).

diverse set of properties (Forman-Kay and Pawson, 1999; Margolis *et al*, 1999). To explore how the ShcA domain associates with IQGAP1$^{401-533}$, we utilized NMR to obtain residue-specific information on this protein–protein interaction. Multi-angle light scattering indicated that the 15 kDa IQGAP1 fragment was monomeric in solution, and CD data that it was α-helical in nature (Supplementary Figure S4). $^{1}H/^{15}N$ heteronuclear single quantum coherence (HSQC) spectra of isotopically labelled IQGAP1$^{401-533}$ also showed the protein to be well-folded. To begin examining its interaction with the PTB domain, we obtained nearly complete backbone resonance assignments for the free PTB domain (residues 17–207) and IQGAP1$^{401-533}$ fragment (86 and 91% respectively) using standard triple resonance experiments (HNCA, HNCACB, and CBCACONH). Upon titration of IQGAP1$^{401-533}$ into ^{15}N-labelled PTB domain we observed significant peak broadening, indicative of an intermediate exchange regime. At low ratios (1 PTB domain:2 IQGAP$^{401-533}$) coalescence appeared specific for particular residues (Figure 6B). Conversely, the titration of unlabelled PTB domain into ^{15}N-labeled IQGAP1$^{401-533}$ yielded specific but more extensive broadening (Figure 6C). These data helped confirm a direct interaction that is distinguished by intermediate exchange on the NMR time-scale, usually indicative of micromolar affinities.

The coalescence observed by this exchange regime is unfortunately detrimental to detailed structural determination. However, data obtained from peak-intensity changes were sufficient to identify a binding interface on the surface of the PTB domain. First, peak intensities derived from HSQC spectra of 300 μM free PTB domain, and PTB domain in the presence of 600 μM IQGAP1$^{401-533}$, were calculated. The ratio (unbound/bound) of all assigned and non-overlapping backbone resonances were plotted (Figure 7A). It was clear that seven peaks exhibited extremely high levels of broadening compared with others (K139, I142, S149, G156, V167, K169, and V172). When mapped on the previously solved structure of the ShcA PTB domain in complex with an NP*X*pY peptide from TrkA (PDB:1SHC; (Zhou *et al*, 1995b)), these residues cluster to a surface region adjacent to the classic peptide-binding groove (Figure 7B). This signified a potentially atypical binding mode for IQGAP1, and we next considered which residues in the IQGAP1 fragment are involved in the interaction.

We carried out a similar peak-intensity analysis on IQGAP1$^{401-533}$ after first establishing an order of 2° structure elements using chemical shift indices (CSI; Figure 7C). This revealed a topology of five α-helices, but suggested helices 1 and 2 may be less well-defined than helices 3–5. Normalized peak intensities from HSQC spectra of 200 μM free

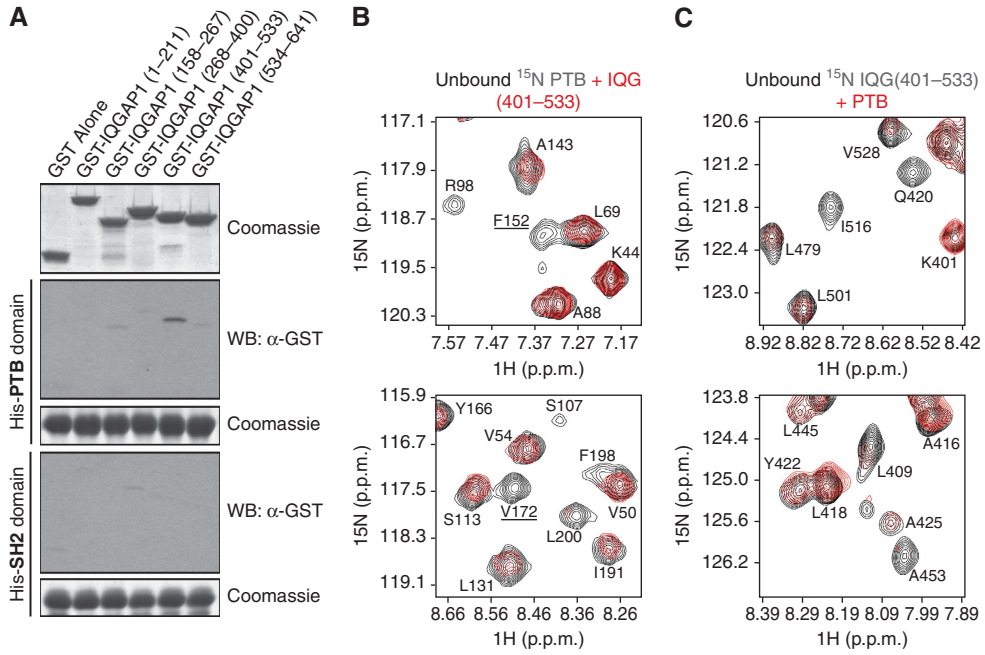

Figure 6 A non-canonical PTB domain interaction with IQGAP1 residues 401–533. (**A**) Determination of PTB domain binding site in IQGAP1 N-terminus. IQGAP1 (residues 1–641) was divided into five segments and expressed as GST-tagged protein (top). His-tagged PTB and SH2 domains bound to Ni-NTA resin were mixed with 2 μM of each IQGAP1 fragment or GST control. Bound proteins were detected by anti-GST immunoblot. (**B**) NMR analysis of the interaction between ShcA PTB domain and IQGAP1$^{401-533}$. Overlay of $^{1}H/^{15}N$ heteronuclear single quantum coherence (HSQC) spectra showing select amide resonances of the ShcA PTB domain in the presence (red) or absence (black) of unlabelled IQGAP1$^{401-533}$ at a 1:2 molar ratio. Several resonances demonstrated high levels of broadening, including F152 (upper) and V172 (lower) (underlined). (**C**) Reverse experiment shows comparable, but more prevalent loss of peak intensities. Overlay of $^{1}H/^{15}N$ HSQC spectra showing select amide resonances from IQGAP1$^{401-533}$ in the presence (red) or absence (black) of unlabelled PTB domain at a 1:4 molar ratio.

IQGAP1$^{401-533}$, and IQGAP1$^{401-533}$ in the presence of 400 μM PTB domain, were calculated and plotted (Figure 7D). We observed a more universal broadening in the IQGAP1 ligand, encompassing most of C-terminal α-helices 3, 4, and 5 (Figure 7E). This provides evidence that the ShcA PTB domain may require more than a short peptide motif to recognize IQGAP1, again suggesting a binding mode that may differ from more conventional NP*X*pY ligands.

ShcA PTB domain interactions with non-pTyr-based ligands

Nearly all ShcA PTB domain ligands contain the NP*X*pY motif, yet one previously identified binding partner is pTyr-independent. This consists of an NPLH sequence in the PTP–PEST phosphatase (Charest *et al*, 1996), an interaction likely analogous to NP*X*pY binding because of conservation of several key residues in the motif (Φ*X*NP*XX*). We therefore examined binding to a PTP–PEST-derived peptide by NMR (PLSFTNPLHSDDWH; Supplementary Figure S5). This peptide bound with a K_d of 6.9 μM as measured by ITC, and associated in the typical β5–α3 groove as determined by comparison with TrkA binding (Farooq *et al*, 2003). Using a molar excess of peptide, 86% of backbone amide resonances were assigned for the NPLH-bound PTB domain (Figure 8A). We next chose to establish if PTB domain binding to the two ligands (NPLH and IQGAP1$^{401-533}$) could happen independently, or was mutually exclusive. To address this, we tested whether an interaction with the NPLH peptide could protect PTB domain amide resonances from exchange broadening induced by IQGAP1$^{401-533}$. Isotopically labelled PTB domain was mixed with NPLH peptide at a 1:5 molar ratio to present two peaks (bound and unbound) of relatively equal intensity. Upon addition of IQGAP1$^{401-533}$ we observed significant coalescence, as before (Figure 8B), but peaks originating from the NPLH-bound PTB domain were not as severely broadened in the residues most involved with binding to IQGAP1$^{401-533}$ (seven obtained from Figure 7A). We measured broadening ratios as a function of peak intensity (unbound/bound) after normalization to maximum signal strength. Figure 8C shows these ratios for free and NPLH-bound PTB domain resonances derived from both highly and more minimally broadened peaks. Data from 12 resonances not substantially affected by IQGAP1$^{401-533}$ (five randomly selected are shown) displayed equal broadening for unbound PTB domain (1.24 ± 0.2) versus NPLH-bound (1.14 ± 0.3), whereas severely broadened peaks (5/7 measurable) showed significantly higher levels for unbound (2.02 ± 0.3) compared with NPLH-bound (1.42 ± 0.3). This suggests that binding to the PTP–PEST peptide conveys a level of protection from the coalescence induced by IQGAP1$^{401-533}$, and that PTB domains occupied in the α3–β5 groove are less likely to interact with IQGAP1.

Discussion

ShcA and IQGAP1 recruitment to surface receptors

We have investigated the possibility that ShcA can signal downstream of activated receptors through pathways other than Grb2–SOS. The absence of Grb2-binding motifs in numerous invertebrate Shc orthologs, and the survival of

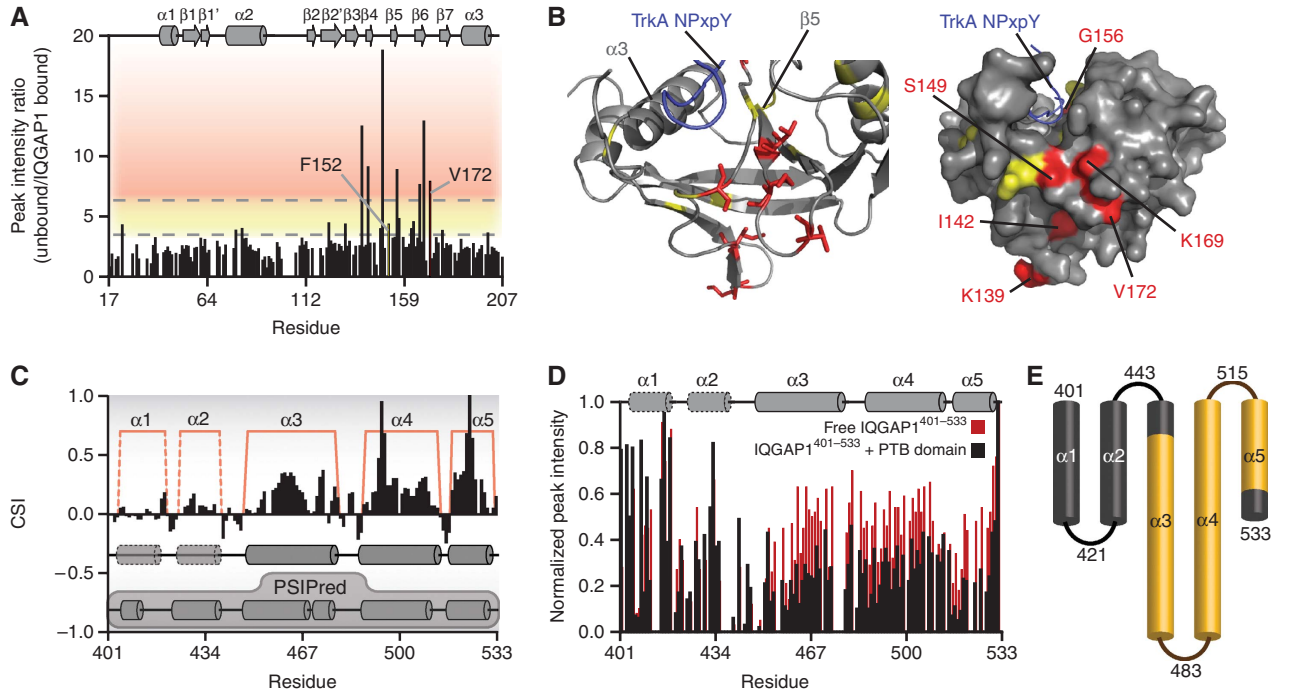

Figure 7 Determination of the PTB domain-IQGAP1 binding interface. (**A**) PTB domain peak intensities in the presence or absence of unlabelled IQGAP1$^{401-533}$ to resolve residues involved in binding (ratio of unbound/bound). A total of 7 resonances were extensively broadened (red zone) and another 12 moderately (yellow zone). Residues F152 and V172, (from Figure 5B), are marked. PTB domain 2° structure elements are at top. (**B**) Structural representation of residues in the ShcA PTB domain that interact with IQGAP1$^{401-533}$. Most broadened amino acids cluster together (left, with structure of PTB domain bound to TrkA; PDB:1SHC (Zhou *et al*, 1995b)). Effected residues are shown in red (highly broadened) or yellow (moderately). The canonical α3–β5 NPXpY-binding groove is marked. The potential-binding interface is also revealed by surface representation (right). (**C**) $^{13}C^{\alpha}$–$^{13}C^{\beta}$ CSI versus residue number for IQGAP1$^{401-533}$. Four consecutive positive CSI values indicate α-helix; four negative values indicate a β-strand. Values indicate fragment is composed of five helices (red outlines on positive region and cylinders below). Helices α1 and α2 are less defined, shown with dashed lines. The PSIPred 2° structure prediction is at bottom. (**D**) $^{1}H/^{15}N$ heteronuclear single quantum coherence (HSQC) peak intensities derived from IQGAP1$^{401-533}$ in the presence or absence of unlabelled ShcA PTB domain to determine ligand-binding region. Peak intensities were normalized to maximum signal strength, and plotted in bound (black) and unbound (red) state. Amide resonances exhibiting significant broadening stand out in red. Representation of IQGAP1$^{401-533}$ from CSI is at top. (**E**) Residues throughout helices α3–α5 exhibit significant broadening. Representation of ligand shows its topological order of 2° structure elements, and highlights regions showing extensive broadening (yellow). Amino acid numbering is from murine IQGAP1.

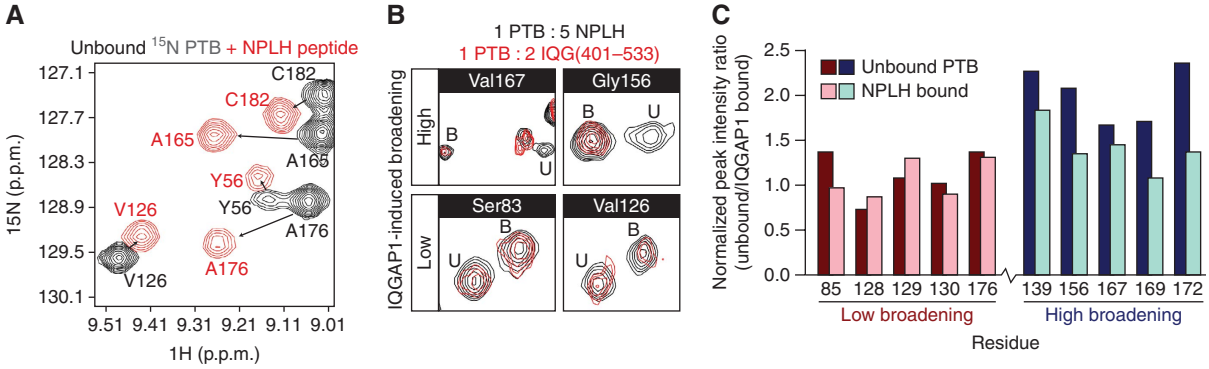

Figure 8 Binding to PTP–PEST peptide and IQGAP1$^{401-533}$ is mutually exclusive. (**A**) Chemical shift perturbations induced by titration of PLSFTNPLHSDDWH peptide. Overlay of $^{1}H/^{15}N$ heteronuclear single quantum coherence (HSQC) spectra showing select PTB domain resonances in the absence (black) or presence (red) of a 1:10 molar ratio of peptide. Arrows indicate movement of resonances upon addition of peptide. (**B**) PTB domain interaction with NPLH peptide imparts protection from IQGAP1-induced broadening. Overlay of spectra showing PTB domain pre-mixed at a 1:5 ratio with NPLH peptide in the presence (red) or absence (black) of unlabelled IQGAP1$^{401-533}$. Two peaks with ordinarily high levels of broadening in the absence of NPLH peptide are shown, as well as two exhibiting lower levels. Resonances derived from unbound PTB domain are marked with 'U', and those from peptide-bound with 'B'. (**C**) Quantitation of peak intensity changes from PTB domain–NPLH complex in the presence or absence of IQGAP1$^{401-533}$. Intensities were normalized to maximum signal strength, and ratio (unbound/bound) plotted for 5/7 peaks that display extensive broadening, and for peaks broadened to a lesser extent (random five selected). Unbound PTB domain data is dark blue or red, and NPLH-bound PTB domain in light blue or red. Average ratio for the typically broadened peaks on the unbound domain (2.02 ± 0.3) is significantly greater than on NPLH-bound (1.42 ± 0.3). Data from 12 other peaks, including the 5 shown, indicate relatively equal broadening (1.24 ± 0.2 unbound versus 1.14 ± 0.3 when NPLH-bound).

ShcA$^{3F/3F}$ mice indicate that alternative signalling pathways are an important component of ShcA function. Both wild type and ShcA^{3F} co-precipitated IQGAP1, a scaffolding protein known to effect cytoskeletal rearrangement (Kuroda *et al*, 1996), the MAPK pathway (Roy *et al*, 2005), Ca^{2+}/calmodulin signalling (Psatha *et al*, 2006), and cadherin/catenin-mediated adhesion (Kuroda *et al*, 1998, 1999). Recent evidence linking IQGAP1 to EGF and PDGF (Blagoev *et al*, 2004; Kratchmarova *et al*, 2005), VEGF (Yamaoka-Tojo *et al*, 2004; Meyer *et al*, 2008), and FGF (Bensenor *et al*, 2007) signalling is consistent with a ShcA interaction, as this adaptor could recruit IQGAP1 to sites where receptors are engaging downstream proteins. Thus, we explored the possibility of a ShcA–IQGAP1 complex, which could have a role in effecting cytoskeletal changes downstream of activated receptors and represents the first steps towards the elucidation of Grb2-independent ShcA signalling.

Our data demonstrate that IQGAP1 is recruited to the cell surface along with ShcA. We detect both ShcA and IQGAP1 at membrane ruffles in fibroblasts expressing constitutively active ErbB2-YD, and both proteins are redistributed to lamellipodia around the edges of 5637 or A431 monolayers stimulated with EGF. This compares well with previous data linking IQGAP1 to insulin-induced ruffles in KB cells (Kuroda *et al*, 1996), VEGF-induced ruffles in endothelial cells (Yamaoka-Tojo *et al*, 2004), and FGF-induced ruffles in MDBK cells (Bensenor *et al*, 2007). We also demonstrate that cells with reduced levels of ShcA are deficient in lamellipodia formation after EGF stimulation, and that IQGAP1 tyrosine phosphorylation is induced by ErbB2 and further augmented by the overexpression of ShcA. Phosphorylation of IQGAP1 seems to be a widespread consequence of growth factor stimulation (Blagoev *et al*, 2004; Yamaoka-Tojo *et al*, 2004; Kratchmarova *et al*, 2005; Bensenor *et al*, 2007), yet the purpose for this remains unknown. As previous work implicated IQGAP1 in activation of Ras/MAPK signalling from the EGFR (Bourguignon *et al*, 2005; Sacks, 2006), we initially considered that its interaction with ShcA could restore some of the activity lost as a result of the 3F/Grb2-binding mutation. However, we have been unable to demonstrate this property of IQGAP1 (Supplementary Figure S6; Roy *et al*, 2004, 2005), and its ability to mediate Ras/MAPK activation through ShcA is still unclear. Instead, we believe the functional significance of ShcA–IQGAP1 redistribution to activated receptors involves cytoskeletal rearrangements mediated by IQGAP1 and Rho family GTPases.

ShcA has previously been implicated in a variety of cytoskeletal-mediated events, specifically cell migration and spreading. Cos7 cells in which ShcA is overexpressed have decreased numbers of actin stress fibres and a motile phenotype (Collins *et al*, 1999). ShcA has also been shown to rapidly associate with the actin cytoskeleton upon stimulation with NGF (Thomas *et al*, 1995), and is thought to influence activation of the Rac1 GEF, Vav1 (Groysman *et al*, 2002; Patrussi *et al*, 2007). *ShcA*$^{-/-}$ embryos display cell–cell adhesion defects in the endothelium at E11.5, and MEFs derived from these mice display a rounded phenotype with abnormal focal complexes and actin stress fibres (Lai and Pawson, 2000). We have preliminary evidence that these MEFs also show a reduction in IQGAP1 recruitment to the cell periphery upon EGF stimulation (M Smith, unpublished data). Most notably, knockdown of ShcA has been suggested to inhibit HRG-dependent migration and lamellipodia formation in ErbB2-YD expressing cells, implying an analogous mechanism to that observed in our EGF-based experiments in 5637 cells (Marone *et al*, 2004). Finally, ShcA has previously been observed in membrane ruffles generated by EGFR/ErbB2 chimeras (Lotti *et al*, 1996). In fact, study of cellular transformation induced by ErbB2, which is amplified in 20–30% of human mammary carcinomas, provides intriguing evidence of Grb2-independent ShcA signalling. Four pTyr sites in the cytoplasmic tail of ErbB2 have potent transforming potential in fibroblasts, two of which recruit Grb2 either directly (YB-Y1144) or through ShcA (YD-Y1226/7) (Dankort *et al*, 1997). However, activated ErbB2 receptors having only the YB or YD sites have distinct abilities to promote epithelial–mesenchymal transition (EMT). Although the YD–ShcA site promotes breakdown of E-cadherin junctions and dispersal of epithelial colonies, the YB–Grb2 site does not (Khoury *et al*, 2001). It is possible that a lack of IQGAP1 recruitment by Grb2 alone is at least partially responsible for the observed decrease in motility and preservation of E-cadherin contacts in ErbB2-YB expressing cells. Indeed, IQGAP1 has been implicated in the metastasis of many cancers (Clark *et al*, 2000; Johnson *et al*, 2009), and has been shown to effect cytoskeletal changes and cadherin-mediated adhesion downstream of growth factor receptors.

IQGAP1 association with VEGFR-2 is the best-characterized link between IQGAP1 and growth factor signalling to date. In a mechanism seemingly distinct from ShcA-mediated IQGAP1 recruitment downstream of ErbB-family receptors, IQGAP1 associates with VEGFR-2 either directly (Yamaoka-Tojo *et al*, 2004) or through a bridging connection mediated by c-Src (Meyer *et al*, 2008). VEGF stimulation results in IQGAP1 phosphorylation and re-distribution to membrane ruffles, which involves activation of Rac1 and breakdown of VE-cadherin-mediated contacts. This corroborates the idea that ShcA–IQGAP1 recruitment to ErbB-family receptors could influence cell shape and motility through Rac1. Rac activation stimulated by growth factor receptors is known to be crucial for lamellipodia formation, cell spreading, and migration, yet the intracellular pathways connecting cell-surface receptors to Rac are still poorly understood. Although activation is achieved by recruiting GEFs such as SOS and Vav2 (Pandey *et al*, 2000; Kurokawa *et al*, 2004; Sini *et al*, 2004), effectors would be essential components for altering cell shape and movement. As IQGAP1 functions to stabilize Rac1 and Cdc42 in their GTP-bound states, and data have shown that it can directly bind and polymerize actin (Bashour *et al*, 1997; Bensenor *et al*, 2007; Le Clainche *et al*, 2007), IQGAP1 should be considered an effector for these GTPases (Zhang *et al*, 1998; Kurella *et al*, 2009). Intriguingly, the presence of IQGAP1 in cells has proven to be an absolute requirement for the proper development of filopodia and lamellipodia (Fukata *et al*, 2002; Le Clainche *et al*, 2007). Indeed, the loss of IQGAP1 signals a decrease in motility for numerous cell types (Bensenor *et al*, 2007; Dong *et al*, 2008; Jadeski *et al*, 2008), and is the likely explanation for the absence of EGF-induced lamellipodia in 5637 cells with reduced levels of ShcA. We can therefore speculate that ShcA-mediated IQGAP1 signalling from growth factor-stimulated receptors leads to Rho-family GTPase activity, directing lamellipodia formation and motility.

The PTB domain of ShcA mediates an interaction with IQGAP1

We have demonstrated a direct, non-canonical interaction between the ShcA PTB domain and IQGAP1 residues 401–533. Several lines of evidence indicate that this ligand is not recognized by a conventional PTB domain-binding mode. Foremost, only an N*XX*F motif near the C-terminus of IQGAP1$^{401-533}$ has any semblance to a PTB domain-binding site, and deletion of this motif did not significantly abolish exchange broadening as observed by NMR (Supplementary Figure S7A/B). We have also been unable to derive any short peptides from this region that are recognized by ShcA (Supplementary Figure S7C/D). Furthermore, an intermediate exchange regime is not typical of ligands binding in the α3–β5 groove (most exhibit slow exchange characteristics (Zhou *et al*, 1995a; Li *et al*, 1998, 2008; Yan *et al*, 2002; Stolt *et al*, 2004)), and at the very least this is indicative of uncharacteristic kinetic properties for this interaction when compared to NP*X*pY-type ligands. Finally, IQGAP1-induced broadening was specific to seven PTB domain resonances that cluster to a region outside of the usual α3–β5 binding pocket. High-resolution structural data are required to determine whether there is an overlap between these sites, but the seven PTB domain residues are completely conserved in four mammalian Shc homologues and in more ancient orthologs. IQGAP1 residues 401–533 are also well conserved (over 90% identity in mammalian IQGAP1s). This suggests preservation of the ShcA–IQGAP1 complex and hints that other Shc proteins may be similarly involved with members of the IQGAP family.

Classical ligands of the NP*X*pY variety bind the ShcA PTB domain with high affinity, having dissociation constants ranging from 53 nM (TrkA pY490) to 5.3 μM (EGFR pY1086) (Zhou *et al*, 1995a). We were unable to resolve an accurate K_d for IQGAP1$^{401-533}$ using ITC, because of highly unfavourable heats of dilution, yet binding appears to be in the high μM range and weaker than NP*X*pY peptides. One intriguing possibility is that this affinity could be augmented by oligomerization of IQGAP1, whereby multiple sites could impart avidity. Data have shown that IQGAP1 exists as a combination of monomers, dimers, and larger oligomers, and that this is dependent on residues in the N-terminal region (763–863) directly adjacent to our identified PTB domain-binding site (Ren *et al*, 2005). Future assays employing larger fragments of the IQGAP1 protein should clarify this.

An NPLH sequence in PTP–PEST, thought to mediate negative regulation of lymphocyte activation (Davidson and Veillette, 2001), was the only previously reported pTyr-independent target for the ShcA PTB domain. The conservation of Asn and Pro in the NPLH sequence suggested binding in the α3–β5 pocket, and comparison of our NMR chemical shift data with published results on TrkA (NP*X*pY) binding (Farooq *et al*, 2003) confirmed this (Supplementary Figure S5C). Competition between this peptide and IQGAP1 demonstrated a mutually exclusive relationship. Owing to the moderate affinity of the NPLH peptide (6.9 μM), the outcome would likely be more pronounced if a high-affinity NP*X*pY ligand were utilized. In fact, one of the seven PTB domain residues involved in the IQGAP1 interaction, Lys169, has a major role in coordinating pTyr recognition (Zhou *et al*, 1995b). Previous data have also shown that the ShcA PTB domain operates by an induced-fit mechanism (Farooq *et al*, 2003). When unbound, residues constituting the ligand-binding pocket in the NP*X*pY-bound form are structurally disordered, and are reorganized in the presence of peptide. This supports the idea that PTB domains engaged in the α3–β5 groove may no longer recognize IQGAP1.

Using the data described here, we propose a model for ShcA recruitment of IQGAP1 to activated receptors. In resting cells, the PTB domain of ShcA could mediate an interaction with IQGAP1 in the cytoplasm. We speculate this complex may be dependant upon oligomerization of IQGAP1, or its further regulation by binding partners such as calmodulin. Upon stimulation, ShcA would be recruited to membrane proximal sites, wherein activated receptors present pTyr residues in the context of NP*X*pY motifs. Owing to a higher PTB domain affinity for these sites, and its inability to associate with the two ligands simultaneously, IQGAP1 would dissociate and begin effecting cytoskeleton rearrangements and breakdown of cell contacts. ShcA would now activate Ras/MAPK through Grb2–SOS, and these signalling complexes can be observed in endosomal compartments where we do not detect IQGAP1.

We have demonstrated alternative modes of ShcA signalling, in which ShcA engages a transient interaction with IQGAP1 and promotes receptor-dependant signalling at lamellipodia. More work is now required to completely characterize the interplay between these proteins, and the functions of this complex in response to various extracellular stimuli.

Materials and methods

Plasmid constructs and antibodies, immunofluorescence, immunoprecipitation, circular dichroism and light scattering procedures are described in Supplementary data.

Cell culture

HEK 293T, Rat1, Madin–Darby canine kidney (MDCK), A431 and 5637 cells were maintained in Dulbecco's modified Eagle's medium containing 10% heat-inactivated fetal calf serum and antibiotics. For exogenous expression, cells were transiently transfected with PEI (Boussif *et al*, 1995), lipofectamine 2000, or lipofectamine LTX (Invitrogen). Selection was done in 1–2.5 μg/ml puromycin (Sigma). EGF (PeproTech) was added after culturing overnight in the absence of serum at indicated times and concentrations. Pervanadate stimulation was for 30 min at 37°C.

Purification of recombinant proteins

Glutathione *S*-transferase or His-tagged proteins were expressed in *E. coli* BL21 cells grown in LB media by induction with isopropyl-b-D-thiogalactopyranoside (IPTG) at 15°C overnight. Cells were lysed and sonicated in 20 mM Tris (pH 7.5), 150 mM NaCl, 10% glycerol, 0.4% NP-40, protease inhibitors (Roche), 1 mM phenylmethylsulfonyl fluoride (PMSF), 10 ng/ml DNase, and either 1 mM dithiothreitol or 10 mM β-mercaptoethanol. Lysate was cleared by centrifugation and incubated with glutathione (Amersham Pharmacia Biotech) or Ni-NTA (Qiagen) resin at 4°C for 2 h. Bound proteins were eluted using 40 mM glutathione (Sigma), 250 mM imidazole (Bioshop), or thrombin cleavage (Calbiochem). Concentrated proteins were purified to homogeneity by size exclusion chromatography using either an S75 or S200 26/60 column (GE Healthcare).

Identification of interacting proteins by mass spectrometry

Rat1 cells were lysed in TX100 buffer (20 mM Tris (pH 7.5), 137 mM NaCl, 10% glycerol, 1% Triton X-100, 1 mM sodium vanadate, 1 mM PMSF, and protease inhibitors) and cleared by ultracentrifugation. Lysate was passed through a 0.45 μm filter (Pall Corporation) and pre-cleared with mouse agarose (Sigma) at 4°C for 30 min. Supernatant was incubated with M2 Flag-agarose (Sigma) for 2 h at 4°C. Beads were washed three times with TX100 buffer before

elution with 1 mg/ml Flag peptide (20 min at RT). After separation by SDS–PAGE, proteins were visualized with colloidal coomassie (GelCode Blue Stain Reagent; Pierce). Bands were excised and reduced, alkylated, and digested with trypsin using a ProGEST Tryptic Digestion Robot (Genomic Solutions). Peptides were analyzed by LC-MS (HP 1100 HPLC System (Agilent) and LTQ Mass Spectrometer (ThermoElectron)). Resultant MS–MS spectra were searched using the MASCOT programme against the NCBI non-redundant DataBase.

Isothermal titration calorimetry (ITC)

Calorimetry experiments were performed using a Microcal VP-ITC instrument. Stock solutions were diluted into filtered and degassed 20 mM Tris (pH 7.5), 100 mM NaCl, and 1 mM DTT. Experiments were carried out at 20°C. Heats of dilution were determined from control experiments in which peptide was titrated into buffer alone. Data were fitted using the software Origin 7 (Microcal).

NMR Spectroscopy

All NMR data were recorded at 25–30°C on an 800 MHz Bruker AVANCE II spectrometer or 600 MHz Bruker AVANCE III spectrometer equipped with TCI CryoProbes. Two-dimensional $^{1}H/^{15}N$ HSQC (Bodenhausen and Ruben, 1980) spectra and triple resonance HNCACB (Wang *et al*, 1994), CBCACONH (Grzesiek and Bax, 1993), and HNCA (Ikura *et al*, 1990) spectra were collected for the backbone chemical shift assignments. All NMR samples were prepared in buffer containing 20 mM Tris (pH 7.5), 100 mM NaCl, 1 mM DTT, and 10% D_2O. Peptide for titrations of sequence 'PLSFTNPLHSDDWH', derived from murine PTP–PEST (ID: 19248), was produced by Sigma. The spectra were processed with NMRPipe (Delaglio *et al*, 1995) and resonance assignments made with NMRView (Johnson, 2004). Backbone assignments have been deposited in the Biological Magnetic Resonance Data Bank with accession codes 16470 and 16471 for NPLH-bound ShcA PTB domain and $IQGAP1^{401-533}$, respectively.

Supplementary data

Supplementary data are available at *The EMBO Journal* Online (http://www.embojournal.org).

Acknowledgements

This work was supported by grants from the Canadian Cancer Society (CCS) (MI) (TP). MJS was a recipient of an Ontario Cancer Institute (OCI) Fellowship. WRH was supported with a CCS studentship. MI holds a Canada Research Chair in Cancer Structural Biology.

Conflict of interest

The authors declare that they have no conflict of interest.

References

Bargmann CI, Weinberg RA (1988) Increased tyrosine kinase activity associated with the protein encoded by the activated *neu* oncogene. *Proc Natl Acad Sci USA* **85:** 5394–5398

Bashour AM, Fullerton AT, Hart MJ, Bloom GS (1997) IQGAP1, a Rac- and Cdc42-binding protein, directly binds and cross-links microfilaments. *J Cell Biol* **137:** 1555–1566

Bates ME, Busse WW, Bertics PJ (1998) Interleukin 5 signals through Shc and Grb2 in human eosinophils. *Am J Respir Cell Mol Biol* **18:** 75–83

Bensenor LB, Kan HM, Wang N, Wallrabe H, Davidson LA, Cai Y, Schafer DA, Bloom GS (2007) IQGAP1 regulates cell motility by linking growth factor signaling to actin assembly. *J Cell Sci* **120:** 658–669

Blagoev B, Ong SE, Kratchmarova I, Mann M (2004) Temporal analysis of phosphotyrosine-dependent signaling networks by quantitative proteomics. *Nat Biotechnol* **22:** 1139–1145

Bodenhausen G, Ruben DJ (1980) Natural abundance ^{15}N NMR by enhanced heteronuclear spectroscopy. *Chem Phys Lett* **69:** 185–189

Bourguignon LY, Gilad E, Rothman K, Peyrollier K (2005) Hyaluronan-CD44 interaction with IQGAP1 promotes Cdc42 and ERK signaling, leading to actin binding, Elk-1/estrogen receptor transcriptional activation, and ovarian cancer progression. *J Biol Chem* **280:** 11961–11972

Boussif O, Lezoualc'h F, Zanta MA, Mergny MD, Scherman D, Demeneix B, Behr JP (1995) A versatile vector for gene and oligonucleotide transfer into cells in culture and *in vivo*: polyethylenimine. *Proc Natl Acad Sci USA* **92:** 7297–7301

Charest A, Wagner J, Jacob S, McGlade CJ, Tremblay ML (1996) Phosphotyrosine-independent binding of SHC to the NPLH sequence of murine protein-tyrosine phosphatase-PEST. Evidence for extended phosphotyrosine binding/phosphotyrosine interaction domain recognition specificity. *J Biol Chem* **271:** 8424–8429

Clark EA, Golub TR, Lander ES, Hynes RO (2000) Genomic analysis of metastasis reveals an essential role for RhoC. *Nature* **406:** 532–535

Collins LR, Ricketts WA, Yeh L, Cheresh D (1999) Bifurcation of cell migratory and proliferative signaling by the adaptor protein Shc. *J Cell Biol* **147:** 1561–1568

Cowan KJ, Law DA, Phillips DR (2000) Identification of shc as the primary protein binding to the tyrosine-phosphorylated beta 3 subunit of alpha IIbbeta 3 during outside-in integrin platelet signaling. *J Biol Chem* **275:** 36423–36429

Dankort D, Maslikowski B, Warner N, Kanno N, Kim H, Wang Z, Moran MF, Oshima RG, Cardiff RD, Muller WJ (2001) Grb2 and Shc adapter proteins play distinct roles in Neu (ErbB2)-induced mammary tumorigenesis: implications for human breast cancer. *Mol Cell Biol* **21:** 1540–1551

Dankort DL, Wang Z, Blackmore V, Moran MF, Muller WJ (1997) Distinct tyrosine autophosphorylation sites negatively and positively modulate *neu*-mediated transformation. *Mol Cell Biol* **17:** 5410–5425

Dans M, Gagnoux-Palacios L, Blaikie P, Klein S, Mariotti A, Giancotti FG (2001) Tyrosine phosphorylation of the β_4 integrin cytoplasmic domain mediates Shc signaling to extracellular signal-regulated kinase and antagonizes formation of hemidesmosomes. *J Biol Chem* **276:** 1494–1502

Davidson D, Veillette A (2001) PTP-PEST, a scaffold protein tyrosine phosphatase, negatively regulates lymphocyte activation by targeting a unique set of substrates. *EMBO J* **20:** 3414–3426

Delaglio F, Grzesiek S, Vuister GW, Zhu G, Pfeifer J, Bax A (1995) NMRPipe: a multidimensional spectral processing system based on UNIX pipes. *J Biomol NMR* **6:** 277–293

Dong PX, Jia N, Xu ZJ, Liu YT, Li DJ, Feng YJ (2008) Silencing of IQGAP1 by shRNA inhibits the invasion of ovarian carcinoma HO-8910PM cells *in vitro*. *J Exp Clin Cancer Res* **27:** 77

Dorsch M, Hock H, Diamantstein T (1994) Tyrosine phosphorylation of Shc is induced by IL-3, IL-5 and GM-CSF. *Biochem Biophys Res Commun* **200:** 562–568

Farooq A, Zeng L, Yan KS, Ravichandran KS, Zhou MM (2003) Coupling of folding and binding in the PTB domain of the signaling protein Shc. *Structure* **11:** 905–913

Finlayson CA, Chappell J, Leitner JW, Goalstone ML, Garrity M, Nawaz S, Ciaraldi TP, Draznin B (2003) Enhanced insulin signaling via Shc in human breast cancer. *Metabolism* **52:** 1606–1611

Forman-Kay JD, Pawson T (1999) Diversity in protein recognition by PTB domains. *Curr Opin Struct Biol* **9:** 690–695

Fukata M, Watanabe T, Noritake J, Nakagawa M, Yamaga M, Kuroda S, Matsuura Y, Iwamatsu A, Perez F, Kaibuchi K (2002) Rac1 and Cdc42 capture microtubules through IQGAP1 and CLIP-170. *Cell* **109:** 873–885

Fukushima A, Hatanaka Y, Chang JW, Takamatsu M, Singh N, Iwashima M (2006) Lck couples Shc to TCR signaling. *Cell Signal* **18:** 1182–1189

Ganju P, O'Bryan JP, Der C, Winter J, James IF (1998) Differential regulation of SHC proteins by nerve growth factor in sensory neurons and PC12 cells. *Eur J Neurosci* **10:** 1995–2008

Gotoh N, Tojo A, Shibuya M (1996) A novel pathway from phosphorylation of tyrosine residues 239/240 of Shc, contributing to suppress apoptosis by IL-3. *EMBO J* **15:** 6197–6204

Gotoh N, Toyoda M, Shibuya M (1997) Tyrosine phosphorylation sites at amino acids 239 and 240 of Shc are involved in epidermal growth factor-induced mitogenic signaling that is distinct from Ras/mitogen-activated protein kinase activation. *Mol Cell Biol* **17:** 1824–1831

Groysman M, Hornstein I, Alcover A, Katzav S (2002) Vav1 and Ly-GDI two regulators of Rho GTPases, function cooperatively as signal transducers in T cell antigen receptor-induced pathways. *J Biol Chem* **277:** 50121–50130

Grzesiek S, Bax A (1993) Amino acid type determination in the sequential assignment procedure of uniformly 13C/15N-enriched proteins. *J Biomol NMR* **3:** 185–204

Hardy WR, Li L, Wang Z, Sedy J, Fawcett J, Frank E, Kucera J, Pawson T (2007) Combinatorial ShcA docking interactions support diversity in tissue morphogenesis. *Science* **317:** 251–256

Hennige AM, Lammers R, Arlt D, Hoppner W, Strack V, Niederfellner G, Seif FJ, Haring HU, Kellerer M (2000) Ret oncogene signal transduction via a IRS-2/PI 3-kinase/PKB and a SHC/Grb-2 dependent pathway: possible implication for transforming activity in NIH3T3 cells. *Mol Cell Endocrinol* **167:** 69–76

Ho YD, Joyal JL, Li Z, Sacks DB (1999) IQGAP1 integrates Ca^{2+}/calmodulin and Cdc42 signaling. *J Biol Chem* **274:** 464–470

Hunt AE, Lali FV, Lord JD, Nelson BH, Miyazaki T, Tracey KJ, Foxwell BM (1999) Role of interleukin (IL)-2 receptor beta-chain subdomains and Shc in p38 mitogen-activated protein (MAP) kinase and p54 MAP kinase (stress-activated protein kinase/c-Jun N-terminal kinase) activation. IL-2-driven proliferation is independent of p38 and p54 MAP kinase activation. *J Biol Chem* **274:** 7591–7597

Ikura M, Kay LE, Bax A (1990) A novel approach for sequential assignment of 1H, 13C, and 15N spectra of proteins: heteronuclear triple-resonance three-dimensional NMR spectroscopy. Application to calmodulin. *Biochemistry* **29:** 4659–4667

Jadeski L, Mataraza JM, Jeong HW, Li Z, Sacks DB (2008) IQGAP1 stimulates proliferation and enhances tumorigenesis of human breast epithelial cells. *J Biol Chem* **283:** 1008–1017

Johnson BA (2004) Using NMRView to visualize and analyze the NMR spectra of macromolecules. *Methods Mol Biol* **278:** 313–352

Johnson M, Sharma M, Henderson BR (2009) IQGAP1 regulation and roles in cancer. *Cell Signal* **21:** 1471–1478

Khoury H, Dankort DL, Sadekova S, Naujokas MA, Muller WJ, Park M (2001) Distinct tyrosine autophosphorylation sites mediate induction of epithelial mesenchymal like transition by an activated ErbB2/Neu receptor. *Oncogene* **20:** 788–799

Kratchmarova I, Blagoev B, Haack-Sorensen M, Kassem M, Mann M (2005) Mechanism of divergent growth factor effects in mesenchymal stem cell differentiation. *Science* **308:** 1472–1477

Kurella VB, Richard JM, Parke CL, Lecour Jr LF, Bellamy HD, Worthylake DK (2009) Crystal structure of the GAP-related domain from IQGAP1. *J Biol Chem* **284:** 14857–14865

Kuroda S, Fukata M, Kobayashi K, Nakafuku M, Nomura N, Iwamatsu A, Kaibuchi K (1996) Identification of IQGAP as a putative target for the small GTPases, Cdc42 and Rac1. *J Biol Chem* **271:** 23363–23367

Kuroda S, Fukata M, Nakagawa M, Fujii K, Nakamura T, Ookubo T, Izawa I, Nagase T, Nomura N, Tani H, Shoji I, Matsuura Y, Yonehara S, Kaibuchi K (1998) Role of IQGAP1, a target of the small GTPases Cdc42 and Rac1, in regulation of E-cadherin-mediated cell-cell adhesion. *Science* **281:** 832–835

Kuroda S, Fukata M, Nakagawa M, Kaibuchi K (1999) Cdc42, Rac1, and their effector IQGAP1 as molecular switches for cadherin-mediated cell-cell adhesion. *Biochem Biophys Res Commun* **262:** 1–6

Kurokawa K, Itoh RE, Yoshizaki H, Nakamura YO, Matsuda M (2004) Coactivation of Rac1 and Cdc42 at lamellipodia and membrane ruffles induced by epidermal growth factor. *Mol Biol Cell* **15:** 1003–1010

Lai KM, Olivier JP, Gish GD, Henkemeyer M, McGlade J, Pawson T (1995) A Drosophila shc gene product is implicated in signaling by the DER receptor tyrosine kinase. *Mol Cell Biol* **15:** 4810–4818

Lai KM, Pawson T (2000) The ShcA phosphotyrosine docking protein sensitizes cardiovascular signaling in the mouse embryo. *Genes Dev* **14:** 1132–1145

Le Clainche C, Schlaepfer D, Ferrari A, Klingauf M, Grohmanova K, Veligodskiy A, Didry D, Le D, Egile C, Carlier MF, Kroschewski R (2007) IQGAP1 stimulates actin assembly through the N-WASP-ARP2/3 pathway. *J Biol Chem* **282:** 426–435

Li H, Koshiba S, Hayashi F, Tochio N, Tomizawa T, Kasai T, Yabuki T, Motoda Y, Harada T, Watanabe S, Inoue M, Hayashizaki Y, Tanaka A, Kigawa T, Yokoyama S (2008) Structure of the C-terminal phosphotyrosine interaction domain of Fe65L1 complexed with the cytoplasmic tail of amyloid precursor protein reveals a novel peptide-binding mode. *J Biol Chem* **283:** 27165–27178

Li SC, Zwahlen C, Vincent SJ, McGlade CJ, Kay LE, Pawson T, Forman-Kay JD (1998) Structure of a Numb PTB domain-peptide complex suggests a basis for diverse binding specificity. *Nat Struct Biol* **5:** 1075–1083

Lotti LV, Lanfrancone L, Migliaccio E, Zompetta C, Pelicci G, Salcini AE, Falini B, Pelicci PG, Torrisi MR (1996) Shc proteins are localized on endoplasmic reticulum membranes and are redistributed after tyrosine kinase receptor activation. *Mol Cell Biol* **16:** 1946–1954

Luttrell LM, Daaka Y, Della Rocca GJ, Lefkowitz RJ (1997) G protein-coupled receptors mediate two functionally distinct pathways of tyrosine phosphorylation in rat 1a fibroblasts. Shc phosphorylation and receptor endocytosis correlate with activation of Erk kinases. *J Biol Chem* **272:** 31648–31656

Mainiero F, Pepe A, Wary KK, Spinardi L, Mohammadi M, Schlessinger J, Giancotti FG (1995) Signal transduction by the alpha 6 beta 4 integrin: distinct beta 4 subunit sites mediate recruitment of Shc/Grb2 and association with the cytoskeleton of hemidesmosomes. *EMBO J* **14:** 4470–4481

Margolis B, Borg JP, Straight S, Meyer D (1999) The function of PTB domain proteins. *Kidney Int* **56:** 1230–1237

Marone R, Hess D, Dankort D, Muller WJ, Hynes NE, Badache A (2004) Memo mediates ErbB2-driven cell motility. *Nat Cell Biol* **6:** 515–522

Mataraza JM, Briggs MW, Li Z, Entwistle A, Ridley AJ, Sacks DB (2003) IQGAP1 promotes cell motility and invasion. *J Biol Chem* **278:** 41237–41245

Mataraza JM, Li Z, Jeong HW, Brown MD, Sacks DB (2007) Multiple proteins mediate IQGAP1-stimulated cell migration. *Cell Signal* **19:** 1857–1865

Mauro L, Sisci D, Bartucci M, Salerno M, Kim J, Tam T, Guvakova MA, Ando S, Surmacz E (1999) SHC-$\alpha_5\beta_1$ Integrin interactions regulate breast cancer cell adhesion and motility. *Exp Cell Res* **252:** 439–448

Meakin SO, MacDonald JI, Gryz EA, Kubu CJ, Verdi JM (1999) The signaling adapter FRS-2 competes with Shc for binding to the nerve growth factor receptor TrkA. A model for discriminating proliferation and differentiation. *J Biol Chem* **274:** 9861–9870

Meyer RD, Sacks DB, Rahimi N (2008) IQGAP1-dependent signaling pathway regulates endothelial cell proliferation and angiogenesis. *PLoS ONE* **3:** e3848

Motegi A, Fujimoto J, Kotani M, Sakuraba H, Yamamoto T (2004) ALK receptor tyrosine kinase promotes cell growth and neurite outgrowth. *J Cell Sci* **117:** 3319–3329

Natarajan K, Berk BC (2006) Crosstalk coregulation mechanisms of G protein-coupled receptors and receptor tyrosine kinases. *Methods Mol Biol* **332:** 51–77

Noritake J, Fukata M, Sato K, Nakagawa M, Watanabe T, Izumi N, Wang S, Fukata Y, Kaibuchi K (2004) Positive role of IQGAP1, an effector of Rac1, in actin-meshwork formation at sites of cell-cell contact. *Mol Biol Cell* **15:** 1065–1076

Pandey A, Podtelejnikov AV, Blagoev B, Bustelo XR, Mann M, Lodish HF (2000) Analysis of receptor signaling pathways by mass spectrometry: identification of vav-2 as a substrate of the epidermal and platelet-derived growth factor receptors. *Proc Natl Acad Sci USA* **97:** 179–184

Patrussi L, Savino MT, Pellegrini M, Paccani SR, Migliaccio E, Plyte S, Lanfrancone L, Pelicci PG, Baldari CT (2005) Cooperation and selectivity of the two Grb2 binding sites of p52Shc in T-cell antigen receptor signaling to Ras family GTPases and Myc-dependent survival. *Oncogene* **24:** 2218–2228

Patrussi L, Ulivieri C, Lucherini OM, Paccani SR, Gamberucci A, Lanfrancone L, Pelicci PG, Baldari CT (2007) p52Shc is required for CXCR4-dependent signaling and chemotaxis in T cells. *Blood* **110:** 1730–1738

Pratt JC, van den Brink MR, Igras VE, Walk SF, Ravichandran KS, Burakoff SJ (1999) Requirement for Shc in TCR-mediated activation of a T cell hybridoma. *J Immunol* **163:** 2586–2591

Psatha MI, Razi M, Koffer A, Moss SE, Sacks DB, Bolsover SR (2006) Targeting of calcium: calmodulin signals to the cytoskeleton by IQGAP1. *Cell Calcium* **41:** 593–605

Ravichandran KS (2001) Signaling via Shc family adapter proteins. *Oncogene* **20:** 6322–6330

Ravichandran KS, Lee KK, Songyang Z, Cantley LC, Burn P, Burakoff SJ (1993) Interaction of Shc with the zeta chain of the T cell receptor upon T cell activation. *Science* **262:** 902–905

Ravichandran KS, Lorenz U, Shoelson SE, Burakoff SJ (1995) Interaction of Shc with Grb2 regulates association of Grb2 with mSOS. *Mol Cell Biol* **15:** 593–600

Ren JG, Li Z, Crimmins DL, Sacks DB (2005) Self-association of IQGAP1: characterization and functional sequelae. *J Biol Chem* **280:** 34548–34557

Ricketts WA, Rose DW, Shoelson S, Olefsky JM (1996) Functional roles of the Shc phosphotyrosine binding and Src homology 2 domains in insulin and epidermal growth factor signaling. *J Biol Chem* **271:** 26165–26169

Roy M, Li Z, Sacks DB (2004) IQGAP1 binds ERK2 and modulates its activity. *J Biol Chem* **279:** 17329–17337

Roy M, Li Z, Sacks DB (2005) IQGAP1 is a scaffold for mitogen-activated protein kinase signaling. *Mol Cell Biol* **25:** 7940–7952

Sacks DB (2006) The role of scaffold proteins in MEK/ERK signalling. *Biochem Soc Trans* **34:** 833–836

Salcini AE, McGlade J, Pelicci G, Nicoletti I, Pawson T, Pelicci PG (1994) Formation of Shc-Grb2 complexes is necessary to induce neoplastic transformation by overexpression of Shc proteins. *Oncogene* **9:** 2827–2836

Sato K, Kimoto M, Kakumoto M, Horiuchi D, Iwasaki T, Tokmakov AA, Fukami Y (2000) Adaptor protein Shc undergoes translocation and mediates up-regulation of the tyrosine kinase c-Src in EGF-stimulated A431 cells. *Genes Cells* **5:** 749–764

Schafer B, Gschwind A, Ullrich A (2004) Multiple G-protein-coupled receptor signals converge on the epidermal growth factor receptor to promote migration and invasion. *Oncogene* **23:** 991–999

Sini P, Cannas A, Koleske AJ, Di Fiore PP, Scita G (2004) Abl-dependent tyrosine phosphorylation of Sos-1 mediates growth-factor-induced Rac activation. *Nat Cell Biol* **6:** 268–274

Sorkin A, McClure M, Huang F, Carter R (2000) Interaction of EGF receptor and grb2 in living cells visualized by fluorescence resonance energy transfer (FRET) microscopy. *Curr Biol* **10:** 1395–1398

Stolt PC, Vardar D, Blacklow SC (2004) The dual-function disabled-1 PTB domain exhibits site independence in binding phosphoinositide and peptide ligands. *Biochemistry* **43:** 10979–10987

Thomas D, Patterson SD, Bradshaw RA (1995) Src homologous and collagen (Shc) protein binds to F-actin and translocates to the cytoskeleton upon nerve growth factor stimulation in PC12 cells. *J Biol Chem* **270:** 28924–28931

Uhlik MT, Temple B, Bencharit S, Kimple AJ, Siderovski DP, Johnson GL (2005) Structural and evolutionary division of phosphotyrosine binding (PTB) domains. *J Mol Biol* **345:** 1–20

van der Geer P, Wiley S, Gish GD, Pawson T (1996) The Shc adaptor protein is highly phosphorylated at conserved, twin tyrosine residues (Y239/240) that mediate protein-protein interactions. *Curr Biol* **6:** 1435–1444

Velazquez L, Gish GD, van Der Geer P, Taylor L, Shulman J, Pawson T (2000) The shc adaptor protein forms interdependent phosphotyrosine-mediated protein complexes in mast cells stimulated with interleukin 3. *Blood* **96:** 132–138

Wang AC, Lodi PJ, Qin J, Vuister GW, Gronenborn AM, Clore GM (1994) An efficient triple-resonance experiment for proton-directed sequential backbone assignment of medium-sized proteins. *J Magn Reson B* **105:** 196–198

Wary KK, Mainiero F, Isakoff SJ, Marcantonio EE, Giancotti FG (1996) The adaptor protein Shc couples a class of integrins to the control of cell cycle progression. *Cell* **87:** 733–743

Watanabe T, Wang S, Noritake J, Sato K, Fukata M, Takefuji M, Nakagawa M, Izumi N, Akiyama T, Kaibuchi K (2004) Interaction with IQGAP1 links APC to Rac1, Cdc42, and actin filaments during cell polarization and migration. *Dev Cell* **7:** 871–883

Weyts FA, Li YS, van Leeuwen J, Weinans H, Chien S (2002) ERK activation and alpha v beta 3 integrin signaling through Shc recruitment in response to mechanical stimulation in human osteoblasts. *J Cell Biochem* **87:** 85–92

Yamaoka-Tojo M, Ushio-Fukai M, Hilenski L, Dikalov SI, Chen YE, Tojo T, Fukai T, Fujimoto M, Patrushev NA, Wang N, Kontos CD, Bloom GS, Alexander RW (2004) IQGAP1, a novel vascular endothelial growth factor receptor binding protein, is involved in reactive oxygen species-dependent endothelial migration and proliferation. *Circ Res* **95:** 276–283

Yan KS, Kuti M, Yan S, Mujtaba S, Farooq A, Goldfarb MP, Zhou MM (2002) FRS2 PTB domain conformation regulates interactions with divergent neurotrophic receptors. *J Biol Chem* **277:** 17088–17094

Zhang B, Chernoff J, Zheng Y (1998) Interaction of Rac1 with GTPase-activating proteins and putative effectors. A comparison with Cdc42 and RhoA. *J Biol Chem* **273:** 8776–8782

Zhou MM, Harlan JE, Wade WS, Crosby S, Ravichandran KS, Burakoff SJ, Fesik SW (1995a) Binding affinities of tyrosine-phosphorylated peptides to the COOH-terminal SH2 and NH2-terminal phosphotyrosine binding domains of Shc. *J Biol Chem* **270:** 31119–31123

Zhou MM, Ravichandran KS, Olejniczak EF, Petros AM, Meadows RP, Sattler M, Harlan JE, Wade WS, Burakoff SJ, Fesik SW (1995b) Structure and ligand recognition of the phosphotyrosine-binding domain of Shc. *Nature* **378:** 584–592

